Isospin-Allowed $O^{16}(d,\alpha)N^{14}$ Differential Cross Sections*

J. E. Jobst†
University of Wisconsin, Madison, Wisconsin
(Received 7 August 1967)

Thin ($\leq$13-keV) gas targets have been used for high-resolution studies of isospin-allowed $O^{16}(d,\alpha)N^{14}$ differential cross sections for $5.0 \leq E_d \leq 9.0$ MeV. Data were taken at six angles for all α groups corresponding to the ground state of N^{14} and excited states at 3.945, 4.91, 5.10, 5.69, 6.23, 6.44, 7.03, and 7.97 MeV. Angular distributions at selected energies were also obtained. Additional survey data at $9.0 \leq E_d \leq 15.0$ MeV were obtained for groups corresponding to the ground state and the 3.945-, 4.91-, and 5.10-MeV excited states at the laboratory angle $\varphi = 14°$; curves were also obtained at $\varphi = 166°$ for the ground-state and 3.945-MeV excited-state groups. There is some evidence for interpreting the observed peaks in the cross section as F^{18} states. Alternatively, even though the level density of F^{18} is perhaps marginal, some of the data were subjected to statistical-fluctuation analysis to check the validity of the $\Gamma/D \sim 2$ criterion. This analysis yielded an average coherence width Γ of the order of 150 keV. Correlation functions with local averages were also tried to test for possible intermediate structure, with negative results. N^{14} levels with $E_x \leq 11.51$ MeV were observed, but no evidence was found for previously reported levels at 6.05, 6.70, 7.40, and 7.60 MeV. The 2.311-MeV first-excited-state, isospin-forbidden α group was also observed, and these data are being separately reported.

INTRODUCTION

THIS paper reports a study of the $O^{16}(d,\alpha_i)N^{14}$ isospin-allowed reactions[1] made simultaneously with the isospin-forbidden reaction reported in a subsequent paper.[2] Differential cross sections of four α groups at six scattering angles will be presented for $E_d = 5.0$–9.0 MeV; less extensive excitation functions will be shown for six additional α groups at three forward angles at energies up to $E_d = 9.0$ MeV. Angular distributions at selected energies will be shown. Some survey cross-section measurements at laboratory scattering angles of 14° and 166° for deuteron energies up to 15 MeV are included.

The $O^{16}(d,\alpha)N^{14}$ reaction has been the subject of considerable earlier research. Lauritsen and Ajzenberg-Selove[3] have reviewed the work prior to 1962. References 4–12 indicate most of the subsequent papers relevant to the present energy range. However, there is a paucity of reliable and extensive cross-section measurements. Browne[13] studied the α_0 and α_2 cross sections for $5.5 \leq E_d \leq 7.5$ MeV in 20-keV energy steps for α_0. He also obtained angular distributions for both groups at $E_d = 7.03$ MeV. Browne's differential cross sections are roughly three times larger than those obtained in the present experiment. However, the α-particle cross sections appearing in the present paper are consistent, in regions of overlap, with the $O^{16}(d,\alpha)$ data of Wright,[14] Messelt,[15] and Jastrzebski *et al.*[4]

EXPERIMENTAL APPARATUS

A tandem Van de Graaff accelerator was used with a small-volume differentially pumped gas scattering chamber.[16] The deuteron beam passed through three pumping impedances before entering the gas scattering chamber. Entrance and exit apertures of diameters 0.152 and 0.114 cm collimated the beam to a half-angle of 12′. The α's were detected by a Si surface-barrier detector which could be rotated about the incident beam direction from 14° to 166° in the laboratory system. The unscattered beam passed through a 0.00010-cm nickel or a 0.00015-cm Havar[17] foil into the collector cup, which was evacuated by a 3.8-cm i.d. orbitron[18] pump. The beam discharged a capacitor which was initially at a known voltage. The null point was detected by a high-gain dc amplifier. Suppression of electrons was achieved by an electrostatic suppressor.

* Work supported in part by the U. S. Atomic Energy Commission.
† Now at EG&G Inc., 680 E. Sunset Road, Las Vegas, Nev.
[1] α_i is defined in Table I.
[2] J. E. Jobst, S. Messelt, and H. T. Richards (unpublished).
[3] T. Lauritsen and F. Ajzenberg-Selove, in *Nuclear Data Sheets*, compiled by K. Way *et al.* (U. S. Government Printing Office, National Academy of Sciences—National Research Council, Washington 25, D. C., 1962).
[4] J. Jastrzebski, F. Picard, J. P. Shapira, and J. L. Picou, Nucl. Phys. **40**, 400 (1963).
[5] T. Yanabu, S. Yamashita, T. Nakamura, K. Takamatsu, A. Masaike, S. Kakigi, D. Ca Nguyen, and T. Takimoto, J. Phys. Soc. Japan **18**, 747 (1963).
[6] J. Cerny, R. H. Pehl, E. Rivet, and B. G. Harvey, Phys. Letters **7**, 67 (1963).
[7] K. A. Gridnev, A. E. Denisov, Yu. A. Nemilov, V. S. Sadkovskii, and E. D. Teterin, Zh. Eksperim. i Teor. Fiz. **46**, 1473 (1964) [English transl.: Soviet Phys.—JETP **19**, 994 (1964)].
[8] T. Honda, H. Horie, Y. Kudo, and H. Ui, Progr. Theoret. Phys. (Kyoto) **31**, 424 (1964).
[9] V. S. Sadkovskii, E. D. Teterin, K. A. Gridnev, A. E. Denisov, R. P. Kolalis, and Yy. A. Nemilov, Yadern. Fiz. **2**, 843 (1965) [English transl.: Soviet J. Nucl. Phys. **2**, 601 (1966)].
[10] V. K. Dolinov, Yu. V. Melikov, and A. F. Tulinov, Zh. Eksperim. i Teor. Fiz., Pis'ma v Redaktsiyu **2**, 120 (1966) [English transl.: Soviet Phys.—JETP Letters **2**, 74 (1966)].
[11] Dai-Ca Nguyen, J. Phys. Soc. Japan **21**, 2462 (1966).
[12] S. Messelt, in *Isobaric Spin in Nuclear Physics*, edited by John D. Fox and Donald Robson (Academic Press Inc., New York, 1966), p. 814.
[13] C. P. Browne, Phys. Rev. **104**, 1598 (1956).
[14] Wright (private communication).
[15] S. Messelt (private communication).
[16] E. A. Silverstein, S. R. Salisbury, G. Hardie, and L. D. Oppliger, Phys. Rev. **124**, 868 (1961); and modifications by S. R. Salisbury, G. Hardie, L. Oppliger, and R. Dangle, *ibid.* **126**, 2143 (1962).
[17] A nickel-chrome alloy obtained from the Hamilton Watch Co.
[18] R. A. Douglas, J. Zabritski, and R. G. Herb, Rev. Sci. Instr. **36**, 1 (1965).

Although the nominal resolution of the detector was about 20 keV, the resolution in the experimental spectra was three to five times larger because of the $\pm 1.85°$ acceptance angle of the collimators. The large acceptance angle was required because of the small cross section of the simultaneously measured isospin-forbidden reaction.[2] A typical pulse-height spectrum with a depletion layer slightly less than the range of the α_0 group is shown in Fig. 1.

For much of the survey data between 9 and 15 MeV, a solid-state counter telescope was used. The dE/dx detector was 35 μ thick and fully depleted at 25 V. A signal from the dE/dx detector was used as a coincidence gate for the added $dE/dx+E$ signal to the analyzer. The lower limit on the gate discriminator was the requirement that elastically scattered deuterons be eliminated from the added signal. The upper limit was set by the additional requirement that the ground-state α group α_0 be included. (At high deuteron energies, the dE/dx loss of α_0 is fairly small.) However, including α_0 on the added spectrum allowed several inelastic deuteron groups to be recorded also. These deuteron groups could be easily identified and usually caused no ambiguity in the identification of α groups. A counter telescope spectrum is shown in Fig. 2.

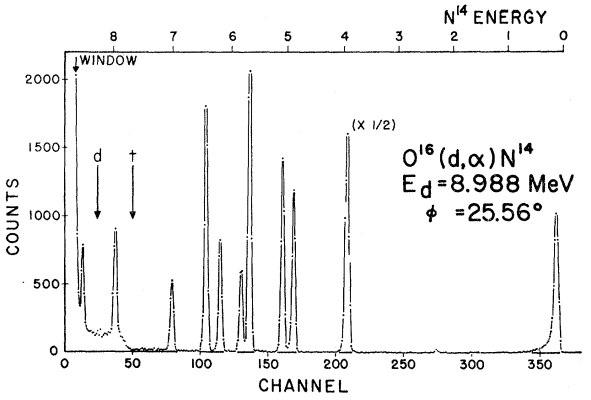

FIG. 1. Typical pulse-height spectrum with the depletion layer slightly less than the range of the α_0 group. The twelve peaks shown are all α groups identified with known states in N^{14}. (The isospin-forbidden α_1 group falls in channel 274.) Data in this paper correspond to all α peaks shown except those associated with $E_x(N^{14})=2.311$ and 8.489 MeV (see Table I). The average α-group width full width at half-maximum (FWHM) is 66 keV; the $\pm 1.85°$ acceptance angle of the detector collimator accounts for an average spread of 62 keV. The peaks in channels 104 and 208 were used for calibration and give the channel width as 22.8 keV. An analyzer bias "window" setting excludes all particles with $E<2.9$ MeV. The maximum pulse height from a deuteron or triton stopped in the depletion layer is indicated by their respective arrows. Proton groups are totally excluded by the window setting. (The highest-energy α group has a low-energy tail and does not correspond exactly to 0 on the N^{14} excitation scale. Both effects result from the fact that these α were not completely stopped in the depletion layer.)

PROCEDURE

This experiment was initially undertaken to study the isospin-forbidden $O^{16}(d,\alpha_1)N^{14*}$ reaction leaving N^{14} in the first excited state.[19] This part of the research program has been extended and is reported in a separate paper.[2] Because of the low α_1 yields much of the data of the present experiment were taken with a gas pressure of 20–25 mm Hg. To accomodate this pressure the oil

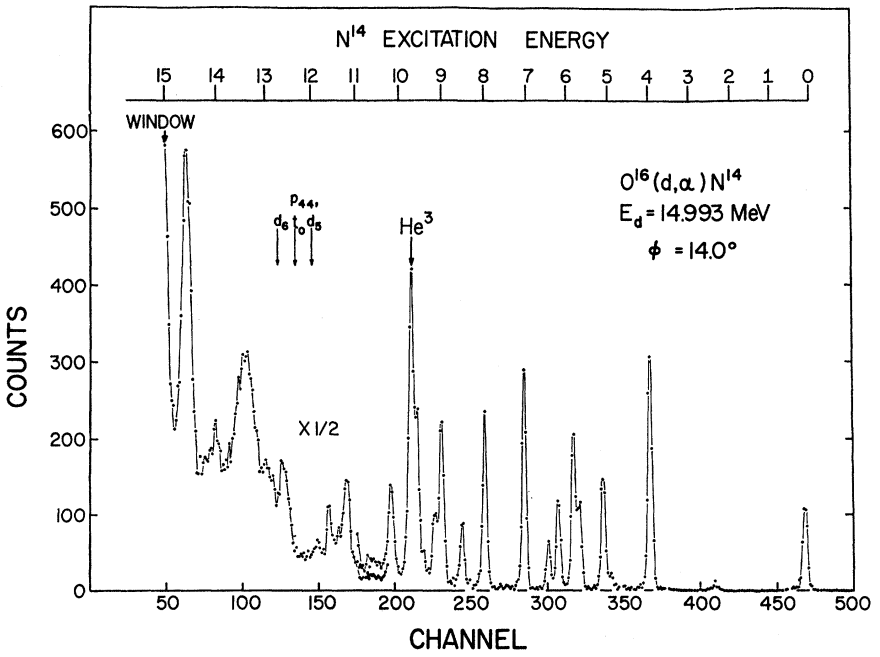

FIG. 2. Typical counter telescope spectrum. The α peaks in channels 368, 301, and 245 (corresponding to N^{14} levels at 3.945, 6.44, and 8.47 MeV, respectively) were used for calibration and give the channel width as 35.1 keV. The group labeled He^3 is from $O^{16}(d,He^3)N^{15}$. The analyzer bias "window" eliminates particles with energies <2.5 MeV. The other arrows indicate possible p, d, or t groups from $O^{16}(d,d_i)O^{16}$, $O^{16}(d,p_i)O^{17}$, and $O^{16}(d,t_i)O^{15}$; the subscript (i) labels the residual nucleus state; no evidence was found for p, d, or t groups of higher energies. Note scale factor ($\times\frac{1}{2}$) for data < channel 180.

[19] J. Jobst, Ph.D. thesis, University of Wisconsin, 1966 (unpublished) (available through University Microfilms, Ann Arbor, Mich.).

manometer was operated as a closed-tube device with an unknown closed-tube volume. α yields obtained in this fashion were calibrated with α cross sections obtained at lower pressures, where the manometer could be used as an open-tube absolute device.

For the E_d=5–9-MeV excitation curves, the bias voltage of the detector was kept very low. These data, shown in Figs. 3–11, were obtained with a single detector. With the depletion layer just thick enough to stop α_0, the deuteron and proton groups lost most of their energy in the insensitive part of the detector. Their small signals in the depleted layer were eliminated by the analyzer bias setting. At high deuteron energies, up to 12 α groups could be observed free of interference from proton or deuteron groups (see Fig. 1).

At some angles and energies α_3 and α_4 were not cleanly separable, nor were α_5 and α_6, and α_8 and α_9. For these cases a computer program called PEAKFIT[20]

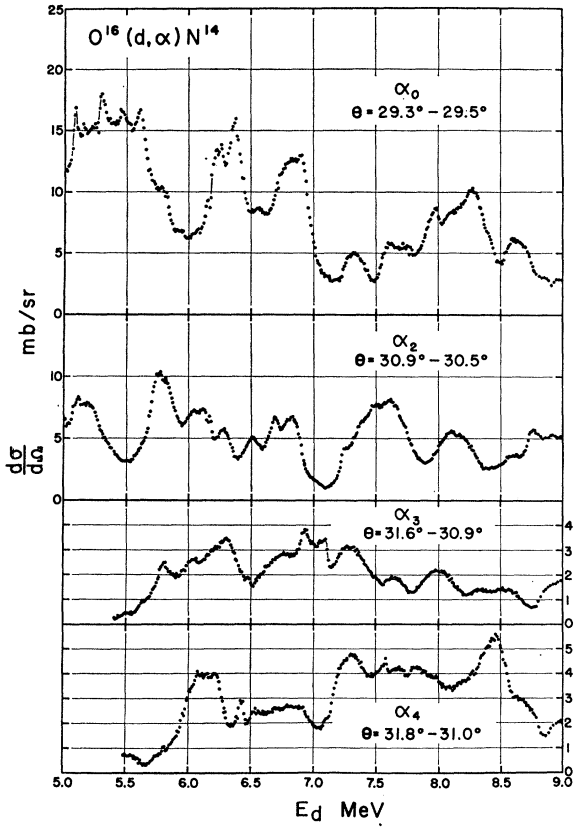

FIG. 3. Excitation curves for α_0, α_2, α_3, and α_4 at $\theta \simeq 30°$. E_d should be reduced by ϵ_d, the energy lost by the deuteron before reaching the center of the target volume; ϵ_d varies from 31 keV at E_d=5 MeV to 12 keV at E_d=9 MeV. Since the laboratory angle was adjusted to keep constant the c.m. angle of the simultaneously recorded α_1 group, θ for the other α groups varies with E_d as indicated.

[20] The original least-squares-data fitting program was obtained from R. H. Moore and R. K. Ziegler, Los Alamos Scientific Laboratory Report No. LA-2367, 1959 (unpublished). The present version was substantially revised and improved by F. deForest, Ph. D. thesis, University of Wisconsin, 1967 (unpublished) (also available through University Microfilms).

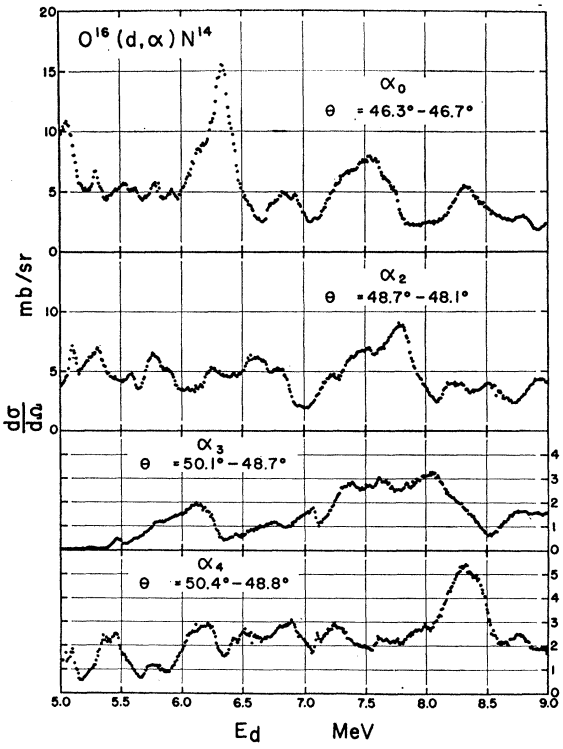

FIG. 4. Excitation curves for α_0, α_2, α_3, and α_4 at $\theta \simeq 48°$. (Also see caption for Fig. 3. For Fig. 4, ϵ_d varies from 19 to 11 keV as E_d increases from 5 to 9 MeV.)

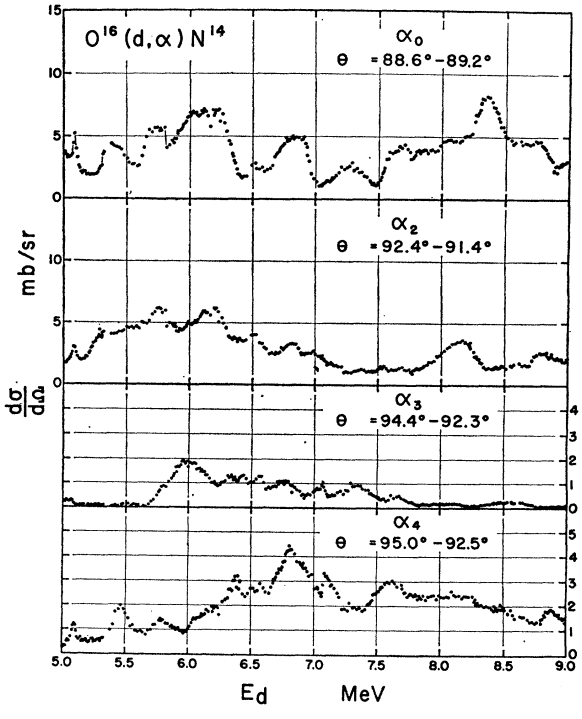

FIG. 5. Excitation curves for α_0, α_2, α_3, and α_4 at $\theta \simeq 91°$. (Also see caption Fig. 3. For Fig. 5 ϵ_d decreases from 19 to 11 keV as E_d increases from 5 to 9 MeV.)

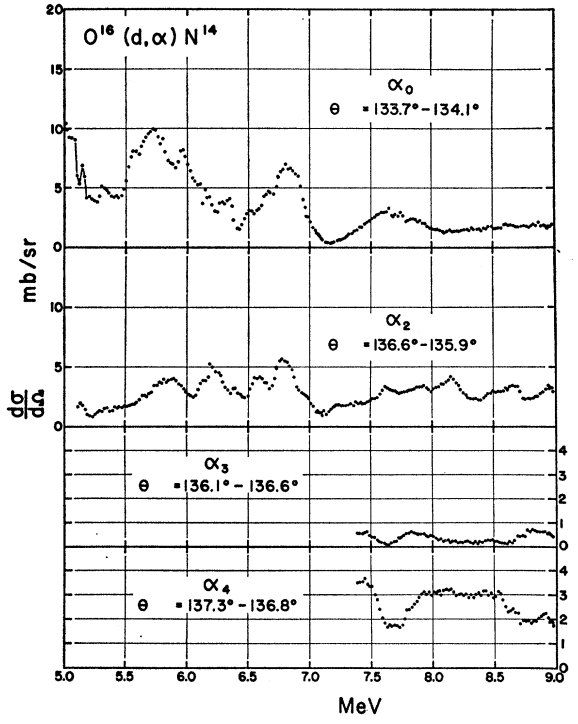

FIG. 6. Excitation curves for α_0, α_2, α_3, and α_4 at $\simeq 135°$. (Also see Fig. 3 caption; for Fig. 6 ϵ_d decreases from 38 to 25 keV as E_d increases from 5 to 9 MeV.)

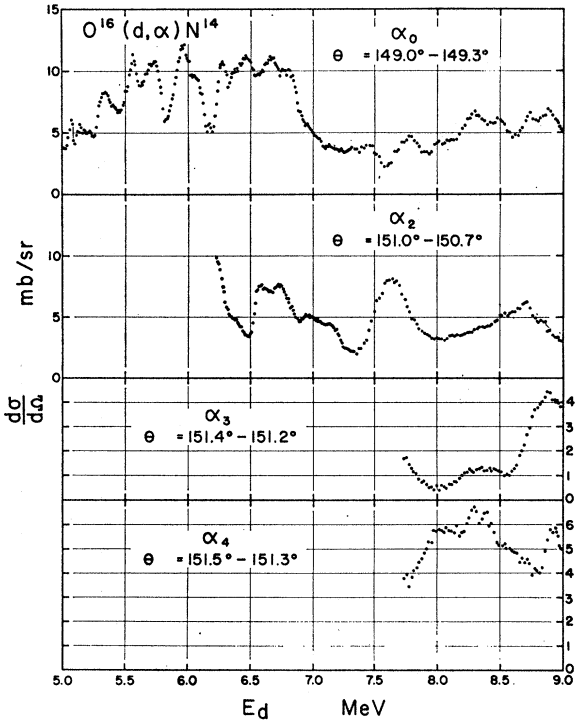

FIG. 7. Excitation curves for α_0, α_2, α_3, and α_4 at $\theta \simeq 150°$. (Also see Fig. 3 caption; for Fig. 7 ϵ_d decreases from 37 to 24 keV as E_d increases from 5 to 9 MeV.)

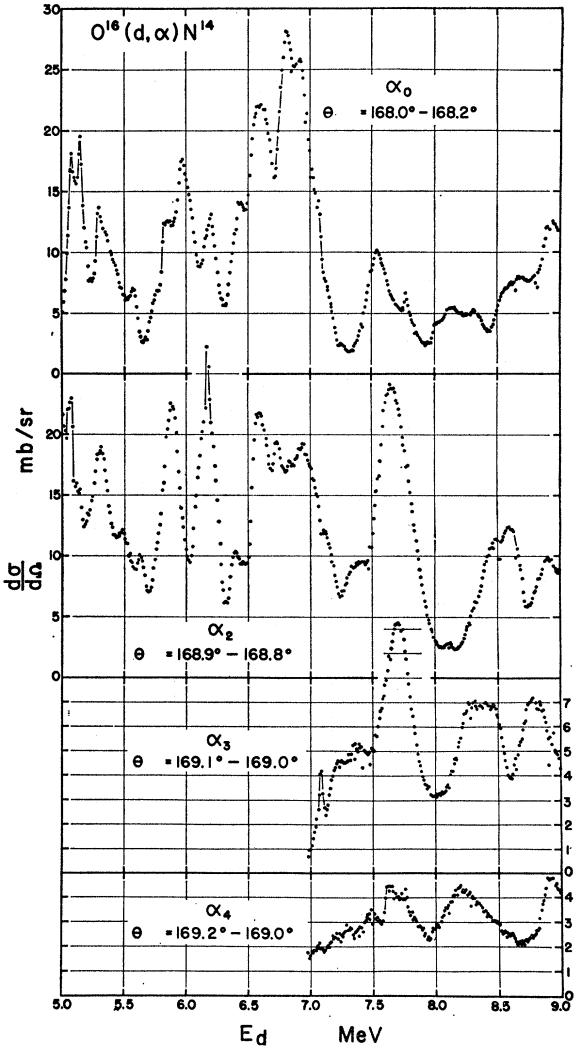

FIG. 8. Excitation curves for α_0, α_2, α_3, and α_4 at $\theta \simeq 168.5°$. (Also see caption Fig. 3; for Fig. 8 ϵ_d decreases from 19 to 10 keV as E_d increases from 5 to 9 MeV.)

was used to fit Gaussian peaks to the observed spectra by the least-squares method and correct for background.

UNCERTAINTIES

The center-of-mass (c.m.) differential cross section is given by

$$\frac{d\sigma}{d\Omega}(\text{c.m.}) = \frac{Y \sin\phi}{NnG}\left(\frac{\sin\phi}{\sin\theta}\right)^2 \cos(\theta-\phi),$$

where

$$\sin(\theta-\phi) = \sin\phi\left[\frac{m_1 m_3}{m_2 m_4}\left(1+\frac{m_1+m_2}{m_2}\frac{Q}{E_d}\right)^{-1}\right]^{1/2}.$$

Y is the number of particles detected, N is the number of incident deuterons, n is the number of target nuclei per cm^3, G is the geometric factor of the counter aperture

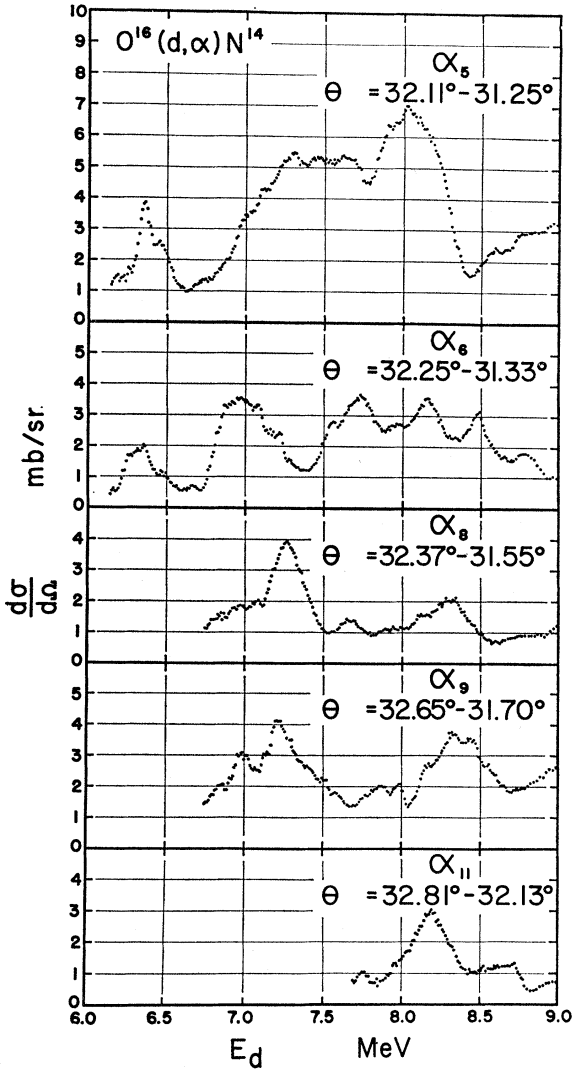

FIG. 9. Excitation curves for α_5, α_6, α_8, α_9, and α_{11} at $\theta \simeq 32.4°$. (See also Fig. 3 caption; for Fig. 9, ϵ_d decreases from 31 to 12 keV as E_d increases from 5 to 9 MeV.)

system,[21] ϕ is the laboratory angle of observation, and θ is the corresponding c.m. angle. $Q=(m_1+m_2)c^2-(m_3+m_4)c^2$, and m_1, m_2, m_3, and m_4 are the masses of the incident projectile, target nucleus, reaction particle, and residual nucleus, respectively. E_d is the laboratory deuteron energy.

The uncertainties are discussed in detail in Ref. 19. Uncertainties of ± 0.3, ± 0.07, and $\pm 0.8\%$ were assigned respectively to N, n, and G. The density n was not corrected for local beam heating, which effect could be $\approx 0.2\%$. The uncertainty in ϕ is $\pm 6'$, which causes an uncertainty of $<\pm 0.7\%$ in the cross sections of the present experiment. For each run the yield Y was obtained by correcting the raw yield for analyzer dead time. There is an additional error of approximately $\pm 0.7\%$ in the dead-time correction factor due to a nonsynchronous live timer in the analyzer. The statistical uncertainty in Y varies from $\pm 0.5\%$ at the largest cross sections to $\pm 25\%$ at the smallest cross sections. The background subtraction introduces an uncertainty in the cross sections of up to $\pm 3\%$ in the lowest 100 keV of the α_2, α_3, and α_4 excitation curves which could not be extended down to 5 MeV. Otherwise the uncertainty due to background subtraction is less than 1%. An additional uncertainty of $<1.5\%$ in n may be present for those data where the closed-tube oil manometer was used for pressure measurement. Hence, systematic uncertainties of ± 2–3% must be added to the statistical uncertainty in the cross section obtained at any given energy. The incident deuteron energy is assigned an uncertainty of ± 15 keV.

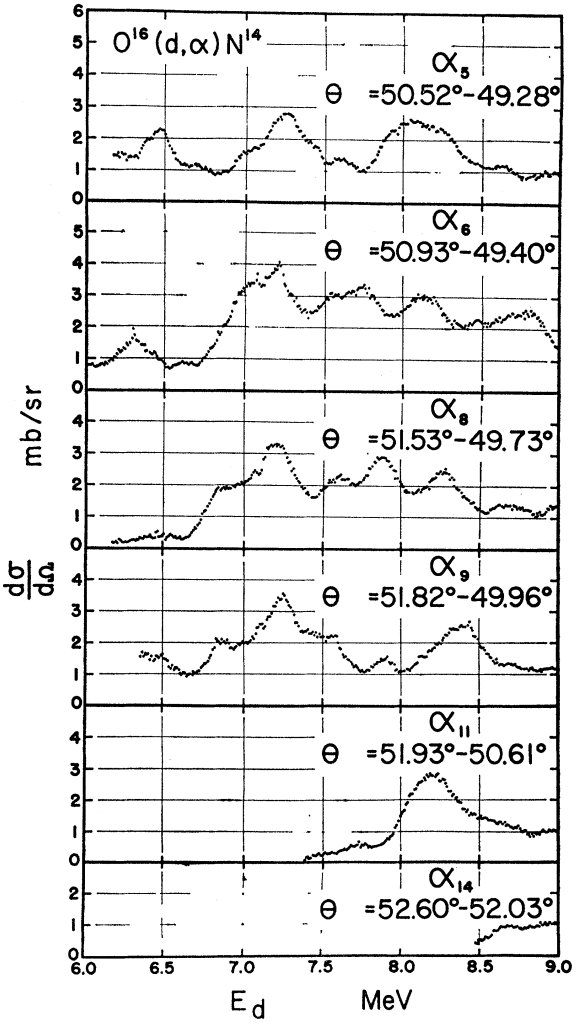

FIG. 10. Excitation curves for α_5, α_6, α_8, α_9, α_{11}, and α_{14} at $\theta \simeq 51°$. (See also Fig. 3 caption; for Fig. 10, ϵ_d decreases from 19 to 11 keV as E_d increases from 5 to 9 MeV.)

[21] E. A. Silverstein, Nucl. Instr. Methods 4, 53 (1959).

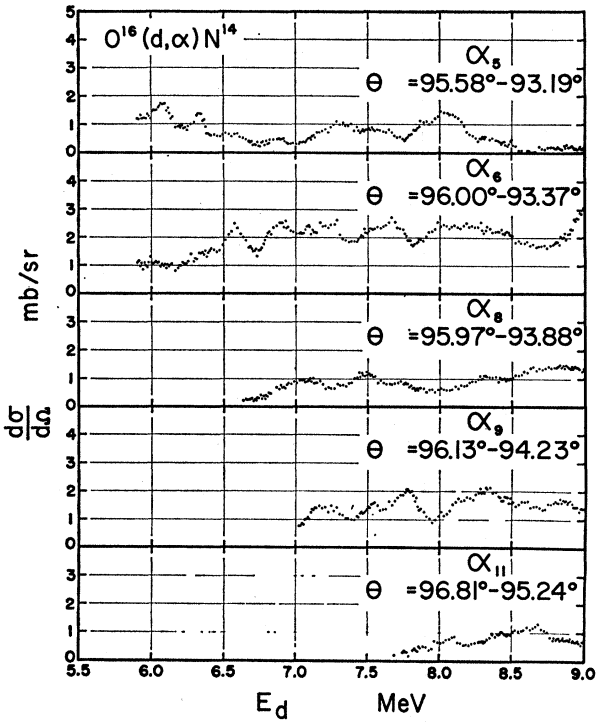

FIG. 11. Excitation curves for α_5, α_6, α_8, α_9, and α_{11} at $\theta \simeq 96°$. (See also Fig. 3 caption; for Fig. 11, ϵ_d decreases from 19 keV at $E_d=5$ MeV to 11 keV at $E_d=9$ MeV.)

Note added in proof. A recent recalibration of the analyzing magnet of the tandem Van de Graaff has shown that values of E_d indicated in this paper are low by $<0.1\%$. Corrections to the deuteron energies indicated in the text and figures are tabulated below.

Indicated E_d (MeV)	Correct E_d (MeV)
5.000	5.019
6.000	6.028
7.000	7.035
8.000	8.044
9.000	9.052
10.000	10.060
11.000	11.068
12.000	12.075
13.000	13.082
14.000	14.087
15.000	15.093

RESULTS

The excitation curves of α_0, α_2, α_3, and α_4 for $5 \leq E_d \leq 9$ MeV are shown in Figs. 3–8. Those for α_5, α_6, α_8, α_9, α_{11}, and α_{14} (see Table I) up to $E_d=9$ MeV are shown in Figs. 9–11; each curve was extended to the lowest energy for which that particular group could be accurately separated from background. Figure 12 shows the data for these groups at back angles. Since the laboratory angle of the detector collimator system was changed to maintain a fixed c.m. angle for the α_1 group, the angle for each of the other groups varied with E_d. The angular range from $E_d=5$ MeV (or the lowest available energy) to 9 MeV is indicated on each excitation curve. The target thickness for all data is ≤ 13 keV. Energy steps are either 10 or 20 keV.

In addition to these excitation curves a series of angular distributions were taken at several energies. The distributions for α_0 and α_2 are shown in Figs. 13 and 14. Those at $E_d \cong 10$ and 11 MeV were taken primarily to determine whether α_0 and α_2 give evidence of a direct reaction mechanism at higher energies. The others were taken at energies where α_1 exhibited resonances.

Both the counter telescope and the single-detector system were used in a coarser survey of the reactions for

TABLE I. Energy levels of final state (N^{14}).

Excitation energy (MeV)	α-group notation	J^π	T	References[a]	Intensity[b] in $O^{16}(d,\alpha)N^{14}$
0	α_0	1^+	0		S
2.311	α_1	0^+	1		W
3.945	α_2	1^+	0	c	S
4.91	α_3	$(0)^-$	0	c	S
5.10	α_4	2^-	0	c	S
5.69	α_5	1^-	0	c	S
5.83	α_6	3^-	0	c	S
(6.05)	α_7			d,e,f,g,h	N
6.23	α_8	$1^{(+)}$	0		S
6.44	α_9	3^+	0	i	S
(6.70)	α_{10}			d,e,g,h	N
7.03	α_{11}	$(2)^+$	0	c	S
(7.40)	α_{12}			d,e,g,h	N
(7.60)	α_{13}			d,e,g,h	N
7.97	α_{14}	2^-	0		S
8.06	α_{15}	1^-	1		I
8.489	α_{16}	4^-	0	j	S
8.617		0^+	1	k	I
8.817		0^-	1	k	I
8.906		3^-	(1)	k	I
8.963		5^+	0	k,j	S
8.979		2^+	(0)	k	
9.129		(2^-)	(0)	j,h	S
9.17		2^+	1		
9.388		$3^-,2^-$	0	k,h	S
9.508		2^-	1	k	S
9.702		1^+	0	k,h	S
10.09		(1^+)	0		S
10.22		1^+	0	h,l	S
10.43		2^+	1		W
10.55		1^-	0	h	I
10.83				h,m	S
11.06		1^+	0		S
11.23		3^-	1	h	S
11.29		2^-	0		
11.39		(1^+)	0		W
11.51		3^+			S

[a] Since the 1962 tabulation of Lauritsen and Ajzenberg-Selove (Ref. 3).
[b] S-strong; W-weak; N-never observed; I-inconclusive evidence.
[c] B. G. Harvey, J. Cerny, R. H. Dehl, and E. Rivet, Nucl. Phys. **39**, 160 (1962).
[d] P. F. Donovan, J. F. Mollenauer, and E. K. Warburton, Phys. Rev. **133**, B113 (1964).
[e] L. G. Earwaker and D. F. Hebbard, Nucl. Phys. **53**, 252 (1964).
[f] Same as Ref. 36.
[g] S. Messelt, Bull. Am. Phys. Soc. **11**, 317 (1966).
[h] Same as Ref. 35.
[i] Hsin-Min Kuan, T. W. Bonner, and J. R. Risser, Nucl. Phys. **51**, 481 (1964).
[j] R. W. Detenbeck, J. C. Armstrong, A. S. Figuera, and J. B. Marion, Nucl. Phys. **72**, 552 (1965).
[k] V. A. Latorre and J. C. Armstrong, Phys. Rev. **144**, 891 (1966).
[l] H. J. Rose, W. Trost, and F. Riess, Nucl. Phys. **44**, 287 (1963).
[m] T. Ishimatsu, S. Morita, T. Tohei, N. Kawai, N. Takano, N. Kato, and Y. Yamanouchi, J. Phys. Soc. Japan **20**, 1112 (1965).

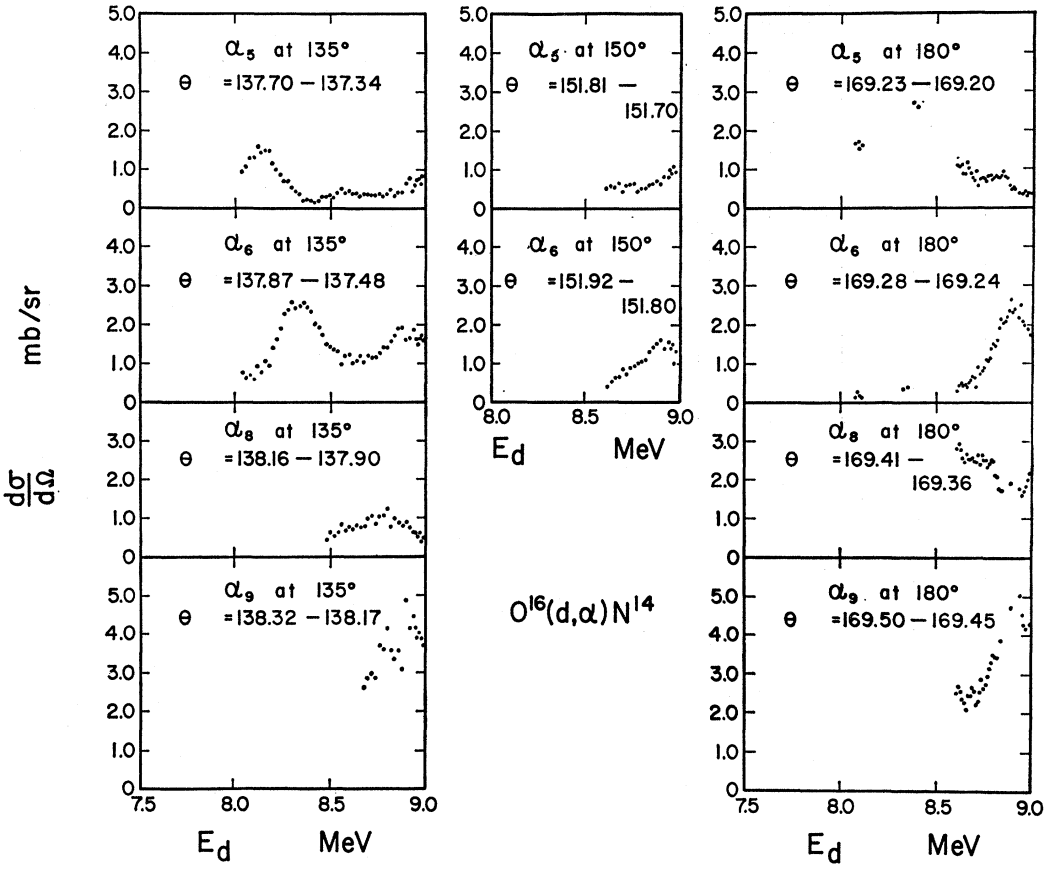

FIG. 12. Excitation curves for α_5, α_6, α_8, and α_9 at back angles. (See also Fig. 3 caption; for Fig. 12, ϵ_d decreases from 38 to 25 keV at 135°, from 37 to 24 keV at 150°, and from 19 to 10 keV at 168° as the energy was increased from 5 to 9 MeV).

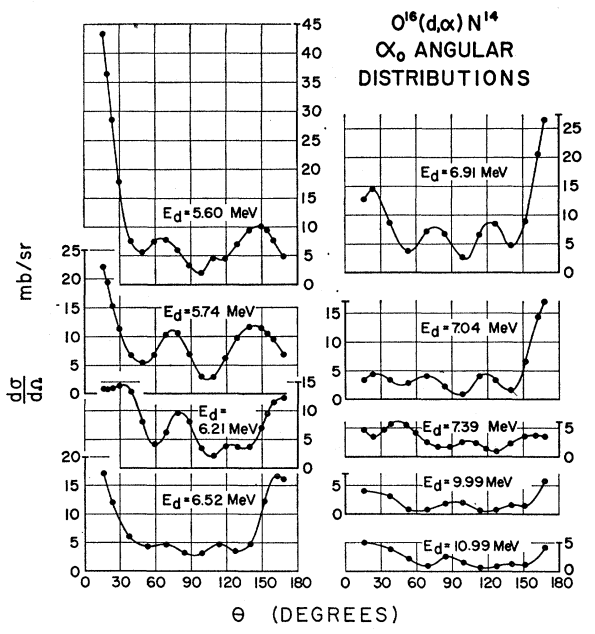

FIG. 13. Angular distribution for α leaving N^{14} in the ground state. Statistical uncertainties are $\leq$ point size.

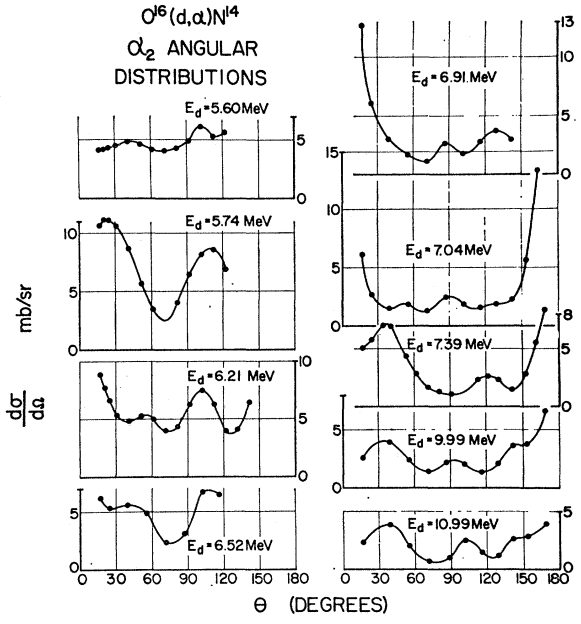

FIG. 14. Angular distributions for α leaving N^{14} in the second excited state (E_x=3.945 MeV). Statistical uncertainties are $\leq$ point size.

$E_d \leqq 15$ MeV at $\varphi = 14°$ and 166°. The forward-angle data are shown in Figs. 15 and 16, the back-angle data in Figs. 17 and 18. For these curves target thickness is ≤ 7 keV. The energy steps range from 1 MeV to 50 keV, except for the region $12.44 \leq E_d \leq 13.56$ MeV at $\varphi = 166°$, which was selected for more detailed study (10-keV steps). Figure 19 shows forward-angle data for α_3 and α_4. The laboratory angles were fixed at $\varphi = 14°$ and 166°; hence θ varied with E_d. All error bars represent statistical uncertainties only. All data are shown as differential cross sections in the c.m. system.

The excitation functions for all ten α groups exhibit fairly strong fluctuations from $E_d = 5$–9 MeV, especially at the forward and backward angles. The angular distributions (see Figs. 13 and 14) give no strong or consistent evidence of forward peaking.

The observed fluctuations could be the result either of individually strong resonances or interference effects from overlapping levels of the same J^π. The latter case has been analyzed in terms of the statistical model of nuclear reaction by Ericson[22] and others.[23,24] Fluctuation

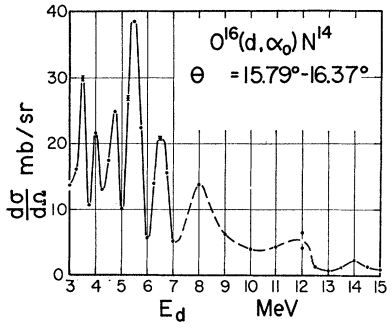

FIG. 15. Forward-angle excitation curve for α_0 at $\phi = 14°$. Statistical uncertainties are shown when they are greater than the point size. E_d is not corrected for loss before reaching the target; these losses range monotonically from 28 keV (at $E_d = 3$ MeV) to 8 keV (at $E_d = 15$ MeV).

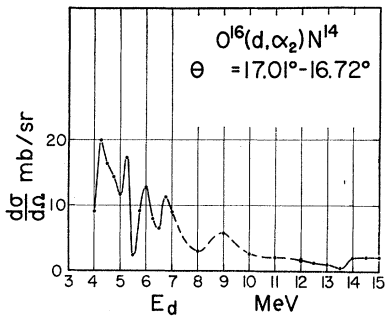

FIG. 16. Forward-angle excitation curve for α_2 at $\phi = 14°$. Statistical uncertainties are smaller than point size. E_d is not corrected for loss before reaching target; these losses range monotonically from 28 keV (at $E_d = 4$ MeV) to 8 keV (at $E_d = 15$ MeV).

[22] T. Ericson, Ann. Phys. (N. Y.) **23**, 390 (1963).
[23] W. R. Gibbs, Los Alamos Scientific Laboratory Report No. LA-3266, 1965 (unpublished).
[24] D. M. Brink and R. O. Stephens, Phys. Letters **5**, 77 (1963).

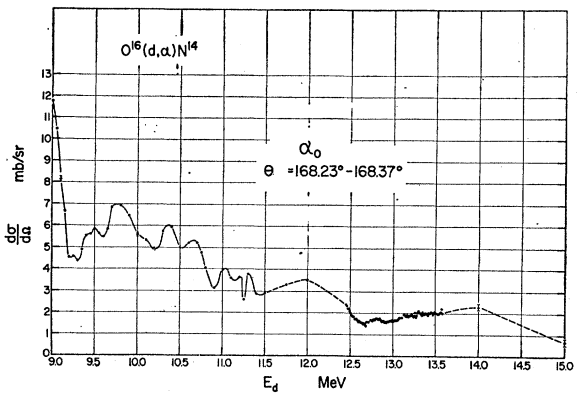

FIG. 17. Excitation curve for α_0 at $\phi = 166°$. The energy scale is not corrected for deuteron energy loss before reaching the target; these losses decrease monotonically from 12 keV (at 9 MeV) to 8 keV (at 15 MeV). Representative statistical errors are shown.

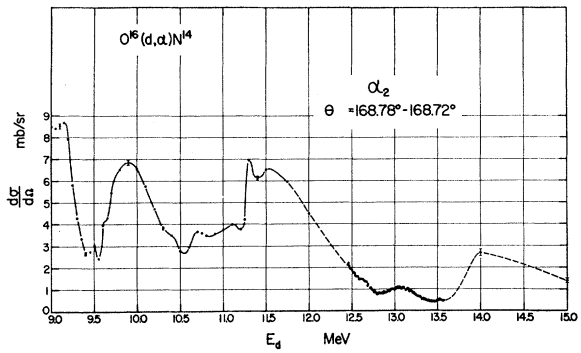

FIG. 18. Excitation curve for α_2 at $\phi = 166°$. The energy scale is not corrected for deuteron energy loss before reaching the target; these losses decreases monotonically from 12 keV (at 9 MeV) to 8 keV (at 15 MeV). Representative statistical errors are shown.

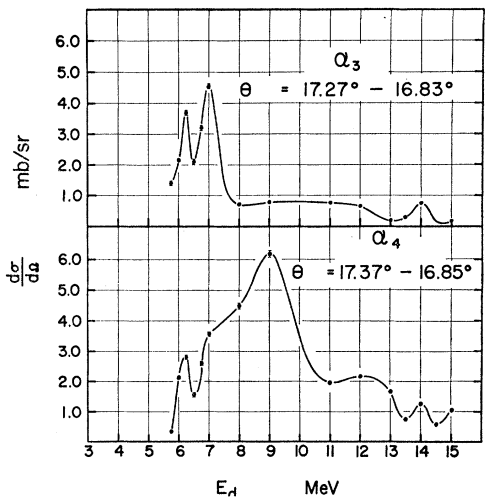

FIG. 19. Forward-angle excitation curves for α_3 and α_4 at $\phi = 14°$. These data were taken simultaneously with that in Figs. 14 and 15. Energy losses range monotonically from 17 keV (at $E_d = 5.75$ MeV) to 8 keV (at $E_d = 15$ MeV).

theory assumes $\Gamma_{J\pi}/D_{J\pi}\gg 1$, where $D_{J\pi}$ is the average level spacing for levels of the same J^π. However, Dallimore and Hall, [25,26] using synthetic excitation functions and equally spaced levels, claim that $\Gamma_{J\pi}/D_{J\pi}\cong 2$ is sufficient to carry out a fluctuation analysis. We may estimate $\Gamma_{J\pi}/D_{J\pi}$ for F^{18} at these excitation energies ($\sim$14 MeV) by using $\langle\Gamma_{J\pi}\rangle\sim 150$ keV from our fluctuation analysis (see Table II) and by using the known spacing of F^{18} levels at low excitation energies (e.g., the 1^+ and 3^+ levels) to fix the constants of a level-density expression suitable for extrapolation to our region of excitation.[27] The latter procedure gives $D_{J\pi}<75$ keV. Hence, $\Gamma_{J\pi}/D_{J\pi}<2$ and the excitation curves of the present experiment may be only marginally adequate for the application of statistical-fluctuation analysis.

If the ratio $\Gamma_{J\pi}/D_{J\pi}$ is marginal for fluctuation-type analysis, then the peaks in the excitation curves may more likely correspond to individual compound nuclear states (F^{18}). Even if interference is important each peak indicates at least one F^{18} level in the neighborhood of the peak. Table III summarizes the average energies, the exit channels, and angles at which there seemed to be pronounced peaks in the cross sections. Also given is the average observed total width (Γ_i) seen at different angles via the ith channel. (These are *not* the partial width for the ith channel.) The variation in the experimental resonance width Γ_i seen via different channels and angles reflects partially the uncertainty in separating close-by states which contribute incoherently; however, the largest variations may arise from true interference effects.

The average experimental width of all the peaks is $\sim$160 keV, which value is consistent with those of Table II obtained from a fluctuation analysis (see below).

FLUCTUATION ANALYSIS

A self-correlation function $C(\epsilon)$ may in principle be related[23] to (1) the average coherence width Γ of the compound level, (2) the effective number N_{eff} of statistically independent channels, and (3) the relative amount of direct interaction y. Thus[28]

$$C(\epsilon)=(1/N_{\text{eff}})(1-y^2)[\Gamma^2/(\Gamma^2+\epsilon^2)].$$

In practice the finite range of data (FRD) effects introduce large corrections and uncertainties to these parameters, especially N_{eff} and y.[29] As a result, the method has not been very useful for extraction of any

TABLE II. Average level widths of F^{18} (11.93–15.5 MeV).

Group	Angle (deg)	n	$C(0)$	N_{eff}	N	Γ_c (keV)	Γ_c(av) (keV)	Γ_k (keV)	Γ_k(av) (keV)	Γ_Δ (keV)	Γ_Δ(av) (keV)
α_0	30	6.1	0.23±0.14	5.3±2.8	5	234±86	198±50	116	133±29	124±46	110±22
	47	9.8	0.25±0.13			139±38		138		135±37	
	90	10.3	0.19±0.10			132±35		147		85±23	
	135	6.3	0.52±0.32			224±80		183		129±46	
	150	5.7	0.15±0.09			251±82		105		(91±30)	
	168	6.8	0.39±0.22			205±69		110		(97±33)	
α_2	30	10.4	0.15±0.09	4.1±3.2	5	131±35	172±132	129	148±36	105±28	115±21
	47	9.6	0.10±0.06			142±40		129		139±38	
	90	3.5	0.24±0.19			438±224		200		(144±74)	
	135	11.1	0.12±0.06			122±31		129		100±25	
	150[a]	10.4	0.11±0.06			89±23		190		98±26	
	168	12.6	0.20±0.09			107±24		116		103±23	
α_3	30	7.1	0.17±0.10	1.2±0.7	2	166±62	231±64[b]	139	181±41[b]	84±31	107±35[b]
	47	4.6	0.40±0.28			293±148		183		147±74	
	90	5.7	0.81±0.50			234±102		220		90±39	
	135	5.9	0.23±0.14			89±38		217		87±37	
	150	3.0	0.53±0.38			147±103		227		55±38	
	168	7.2	0.13±0.08			92±34		92		110±40	
α_4	30	7.2	0.17±0.10	4.8±3.0	8	177±53	209±50[b]	128	143±52[b]	122±37	95±27[b]
	47	7.9	0.18±0.09			183±52		100		95±27	
	90	5.7	0.21±0.13			267±89		200		(69±23)	
	135	5.5	0.05±0.04			109±37		145		84±29	
	150	4.7	0.02±0.01			105±39		170		96±35	
	168	7.1	0.07±0.05			105±32		138		107±32	

[a] Excitation curve for $6.25\leq E_d\leq 9.0$ MeV.
[b] Only 30°, 45°, and 90° data included.

[25] P. J. Dallimore and I. Hall, Phys. Letters **18**, 138 (1965).
[26] P. J. Dallimore and I. Hall, Nucl. Phys. **88**, 193 (1966).
[27] M. A. Preston, *Physics of the Nucleus* (Addison-Wesley Publishing Co., Inc., Reading, Mass., 1962), p. 528.
[28] According to W. R. Gibbs (Ref. 23) a proof of this statement is given by R. O. Stephen in his Ph.D. thesis, Oxford, 1966 (unpublished).
[29] A. Van der Woude, Nucl. Phys. **80**, 14 (1966).

TABLE III. Cross-section maxima interpreted as individual F^{18} states.

Incident deuteron energy E_d (MeV)	F^{18} excitation energy (MeV)	Resonance widths (in keV)[a] Γ_0	Γ_1	Γ_2	Γ_3	Γ_4
5.03	11.63					45-b
5.08	12.03	78-abcef		67-bcf		48-bc
5.15	12.09	60-df				
5.30	12.26	80-bf				
5.32	12.24	174-ade		210-f		
5.38	12.30	175-c				130-b
5.44	12.35		68-ab			100-b
5.46	12.38			120-f	90-b	140-c
5.56	12.45	145-bef	78-ef	170-b		
5.62	12.50	210-a	118-acd	130-f		
5.74	12.61	187-cde				
5.77	12.65	208-abf		158-abc		200-c
5.79	12.66		65-abcdef		100-a	70-a
5.88	12.74			182-bf		
5.97	12.82	140-def				
6.08	12.92	170-e	93-ef			150-a
6.11	12.95		113-abc			
6.16	12.99			185-f	280-b	
6.22	13.04	160-cf				170-ab
6.22	13.04		40-a			
6.27	13.09	110-e		240-ab		
6.28	13.10		40-a			
6.31	13.12	140-d			220-a	
6.35	13.16	178-ab			140-c	
6.37	13.17		68-cef			
6.40	13.20			135-f		
6.43	13.23	150-f	83-ab			102-ab
6.51	13.30		68-aef			
6.51	13.30	120-d		175-ac		
6.58	13.36		100-d	153-def	140-c	140-c
6.61	13.39	180-f		270-b		
6.66	13.43	150-e	95-a			
6.69	13.46			115-a		
6.72	13.49		65-bc			
6.73	13.49			138-ef		
6.77	13.53		107-ef	155-d	210-c	
6.81	13.57	170-def		158-abc		180-c
6.91	13.66	105-abcf	62-aef		100-a	
7.08	13.81		178-bdef			
7.08	13.81				58-abcf	75-bcf
7.15	13.87		230-c			
7.23	13.94		170-b		160-f	
7.26	13.97			120-a		
7.30	14.00	290-c	200-e		280-a	220-a
7.34	14.04	245-a	205-bd		240-c	
7.39	14.08		190-a		350-b	
7.45	14.13	240-e				
7.54	14.21	220-f				
7.58	14.25					95-a
7.62	14.28	160-a		160-d		110-bf
7.63	14.30	265-cd		280-aef	270-a	320-c
7.69	14.35		160-d			
7.70	14.36				260-f	
7.76	14.41	75-f				80-f
7.78	14.43	280-e		230-b		
7.81	14.45		113-ef			
7.95	14.58					220-d
7.98	14.60	170-a				
7.99	14.61				340-a	
8.03	14.65	110-f	150-a			
8.04	14.66				320-b	350-e
8.09	14.71		200-d			
8.11	14.72		100-f			
8.17	14.77			280-c		
8.12	14.80					420-f
8.26	14.86	220-a		260-b	225-ef	
8.30	14.89					125-e
8.33	14.92	160-f	130-a			
8.33	14.92	340-b			220-a	
8.36	14.94	350-c				
8.39	14.97		140-b			125-e
8.46	15.03				225-ef	190-a
8.48	15.05			170-f		
8.51	15.08			240-b		
8.51	15.08		80-a			
8.53	15.10					200-d
8.56	15.12	180-f			260-a	
8.60	15.16	130-a		170-f		
8.67	15.22			150-d		130-d
8.71	15.25			180-e		
8.74	15.28	220-e				
8.77	15.31	300-bc			222-bf	260-b
8.84	15.37				120-f	
8.88	15.41				220-e	200-c
8.92	15.44			280-bf		190-def
8.95	15.47	240-f	240-f	140-d		

[a] Γ_i is the width in keV as seen via the ith channel (or average width if the level is observed at several angles) of a comparatively well-resolved peak in the α_i excitation curve at the indicated deuteron energy E_d (see Figs. 3–8). The letters indicate the angles at which the peaks appeared, according to the following code: a, 30°; b, 45°; c, 90°; d, 135°; e, 150°; and f, 168°.

parameter except Γ. The latter quantity is usually obtained from the self-correlation function[30]

$$C(\epsilon)=\frac{\langle\sigma(E+\epsilon)\sigma(E)\rangle}{\langle\sigma(E+\epsilon)\rangle\langle\sigma(E)\rangle}-1$$

by setting $C(\Gamma)=\frac{1}{2}C(0)$. The coherence width Γ may also be found by counting the number of cross-section maxima per unit energy range.[24,25] A recent analysis of fluctuations in synthetic excitation functions[29] indicates that the peak-counting technique is perhaps more reliable than the autocorrelation method and confirms the general experience that none of the techniques is very useful for fixing N_{eff} or y.

[30] B. W. Allardyce, W. R. Graham, and I. Hall, Nucl. Phys. 52, 239 (1964).

The excitation curves for α_0, α_2, α_3, and α_4 have been analyzed with both techniques. Fluctuation analysis has not been performed on α_5, α_6, α_8, α_9, α_{11}, or α_{14}. These excitation curves are generally too short to be expected to yield reliable results. For the autocorrelation method, the energy increment ϵ was varied from 0–2000 keV. Typical correlation functions are shown in Fig. 20. The calculated $C(\epsilon)$ generally oscillates about the axis due to FRD effects.[30] These FRD effects are strong for the present data because the sample size, $n=R/\pi\Gamma+1$, is usually quite small[23] (R is the energy range of the data).

The widths Γ can be corrected for FRD effects. If $y=0$, then the corrected width Γ_c becomes[23]

$$\Gamma_c=\Gamma[(n-1)(4n-4+N)/4n^2]^{1/2}.$$

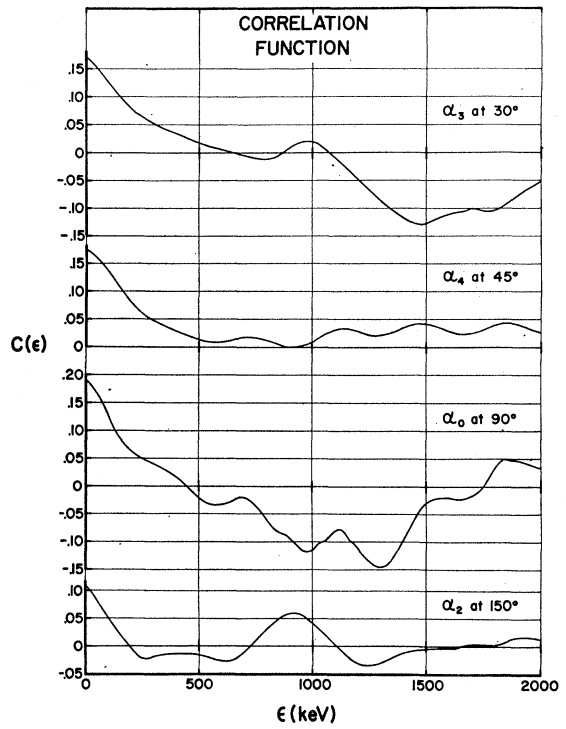

FIG. 20. Typical correlation function $C(\epsilon)$. The coherence width Γ_c is obtained from the initial dropoff of $C(\epsilon)$, i.e., $C(\Gamma)=\frac{1}{2}C(0)$. The Γ's obtained from these curves are (from top to bottom, uncorrected for FRD effects) 186, 185, 137, 93, and 52 keV.

The values of $C(0)$, n, and Γ_c calculated from the data of Figs. 3–8 are shown in Table II. The uncertainties were calculated from the formulas and graphs of Ref. 23.

Table III also includes an estimate of the coherence width from peak counting. This width we denote by Γ_k and is related to the number of maxima per unit energy interval k by[25,26] $\Gamma_k=0.55/k$. The uncertainty in Γ_k (average) is the standard deviation about the mean.

It will be observed that Γ_k is systematically smaller than the corresponding Γ_c. This result is opposite to that observed by Van der Woude[29] from an analysis of synthetic excitation functions and may reflect the fact that $\Gamma_{J\pi}$ is not $\gg D_{J\pi}$. Large uncertainties are involved in both methods. But it would appear that counting peaks gives as satisfactory an estimate of Γ as does the more elaborate correlation analysis.

LOCAL AVERAGING METHOD

There have been recent suggestions[31] that structures may exist in nuclear reaction cross sections which are intermediate between the width of compound-nucleus levels and the width of the optical-model giant resonances. Gadioli *et al.*[32] and Pappalardo[33] suggest that one can discriminate between such intermediate structures and fluctuations from the statistical model by using an autocorrelation function with a moving local average:

$$C(\Delta,\epsilon)=\langle(\sigma(E)/\sigma_\Delta(E)-1)(\sigma(E+\epsilon)/\sigma_\Delta(E+\epsilon)-1)\rangle,$$

where $\sigma_\Delta(E)$ is the local average cross section. The brackets again denote an average over the full energy range.

We have also calculated such correlation functions for our data. The coherence width Γ_Δ is calculated by fixing Δ, varying ϵ from 0–2000 keV, and using the relation

$$C(\Delta,\Gamma_\Delta)=\tfrac{1}{2}C(\Delta,0).$$

A major difficulty in this procedure is proper choice of the averaging interval Δ. Under the assumption that a given cross section has structures of two definite sizes (i.e., narrow widths due to Ericson fluctuations and wide ones due to intermediate resonances), Pappalardo[33] suggests that the curve $C(\Delta,0)$, plotted as a function of Δ, will behave in the following manner.

If Δ is smaller than the width of the statistical fluctuations, the average cross section σ_Δ "follows" (and smooths out) these fluctuations. Then $C(\Delta,0)$ will be small but increase rapidly with Δ. When Δ is larger than the width of the narrow statistical fluctuations, Γ_Δ, then $C(\Delta,0)$ will be independent of Δ. When Δ is larger than the widths of any intermediate structure, $C(\Delta,0)$ should increase rapidly again.

The functions $C(\Delta,0)$ and $\Gamma(\Delta)$ were calculated for each excitation function in Figs. 3–8. Each point on $\Gamma(\Delta)$ is Γ_Δ, calculated from $C(\Delta,\epsilon)$ for the given Δ. Figure 21 shows three examples of $C(\Delta,0)$ and $\Gamma(\Delta)$ curves. Those for α_4 at 30° are fairly typical of the majority of the excitation functions. A plateau in $C(\Delta,0)$ is usually accompanied by one in $\Gamma(\Delta)$; the onset of the $\Gamma(\Delta)$ plateau usually occurs for a Δ smaller by 100–600 keV than that at which the $C(\Delta,0)$ plateau begins.

The character of both the $C(\Delta,0)$ and $\Gamma(\Delta)$ curves is not well understood. However, for $\Delta\sim2000$ keV, the FRD effects became so important that the curves become meaningless. A plateau in $\Gamma(\Delta)$ was considered significant if it was ~400 keV wide, if it started at $\Delta<2000$ keV, and if

$$|\Gamma_{\Delta i}-\Gamma_\Delta(\mathrm{av})|/\Gamma_\Delta(\mathrm{av})\leq10\%$$

for all Δ_i within the plateau. If $\Gamma(\Delta)$ exhibited more than one plateau, that corresponding to the lowest range of Δ_i was considered pertinent to the average Ericson fluctuation width. For most cases plateaus were much larger than 400 keV and the $\Gamma_{\Delta i}$ deviated much less than 10% from the average value.

[31] B. Bloch and H. Feshbach, Ann. Phys. (N. Y.) **23**, 47 (1963).

[32] E. Gadioli, G. M. Marcassan, and G. Pappalardo, Phys. Letters **11**, 130 (1964).

[33] G. Pappalardo, Phys. Letters **13**, 320 (1964).

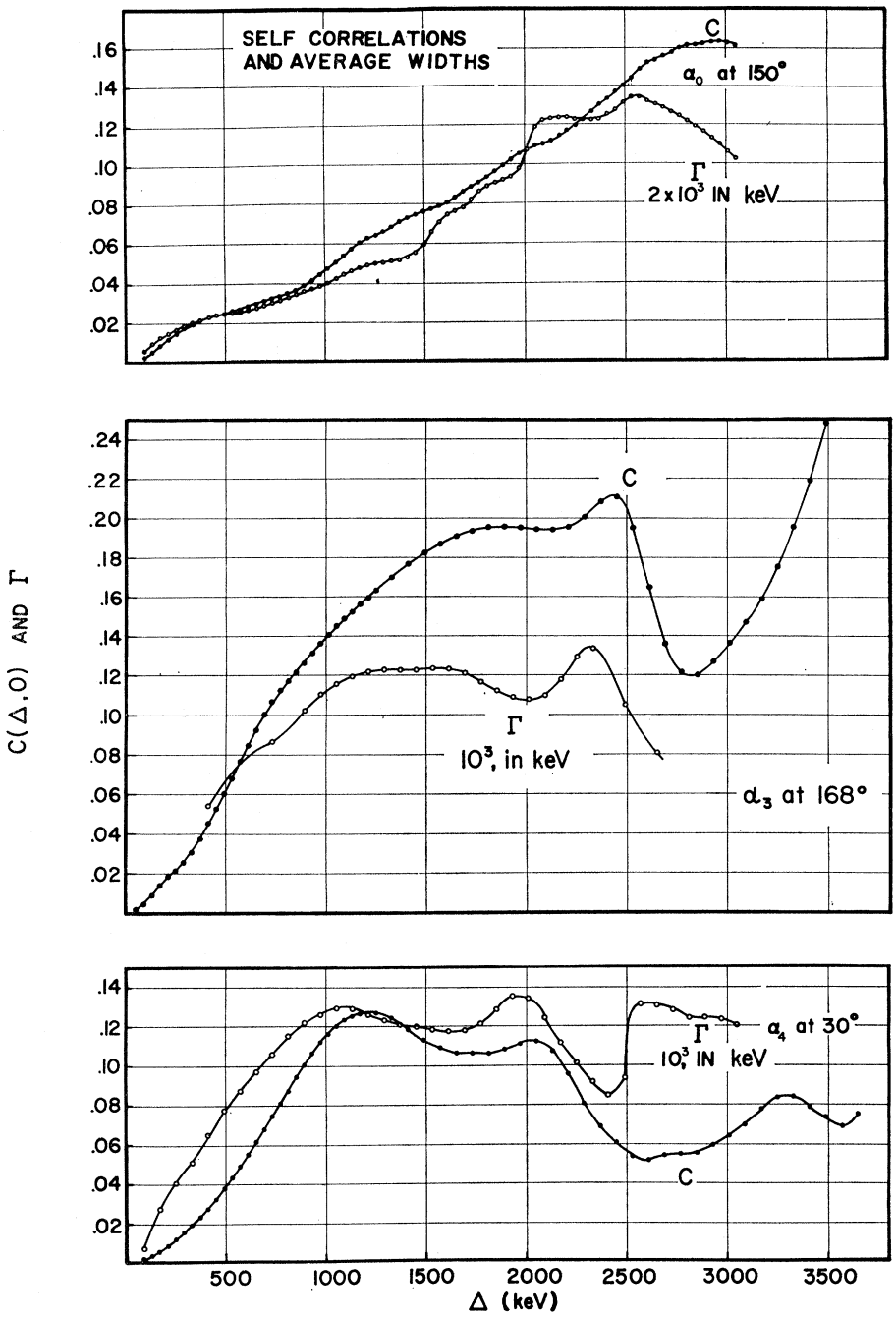

FIG. 21. Typical graphs of $\Gamma(\Delta)$ are superposed on the corresponding $C(\Delta,0)$ curves. Since $C(\Delta,0)$ is dimensionless, the ordinate is converted to keV for $\Gamma(\Delta)$ when multiplied by the scale factor immediately below each $\Gamma(\Delta)$ curve. For example, the maximum calculated width $\Gamma(\Delta)$ for α_0 at 150° (at $\Delta\sim2550$ keV) is $\Gamma=0.135\times2\times10^3=270$ keV.

If a plateau satisfied the above criteria, all $\Gamma_{\Delta i}$ within it were averaged; this average value was corrected for sample-size effects using the formula of Gibbs[23] and is shown in Table II as Γ_Δ. The indicated uncertainties are FRD effects and were calculated from the fractional uncertainty in the corresponding Γ_c.[34] For α_2, Γ_Δ(av) overlaps Γ_c (av); for α_0, α_3, and α_4, Γ_Δ(av) is significantly smaller. The uncertainty in Γ_Δ(av) is again the standard deviation about the mean.

In some cases the $C(\Delta,0)$ curve shows no plateau at all for $\Delta<2500$ keV, e.g., $C(\Delta,0)$ for α_0 at 150° in Fig. 21. This result could imply that the level widths for that group and angle vary continuously from very small to very large values. In most such cases, however, there is either a very short plateau or perhaps just a change in the slope of the $\Gamma(\Delta)$ graph, e.g., the region

[34] This procedure may give an underestimate of the uncertainty in Γ_Δ since the Δ_i corresponding to the plateau (the ranges over which the σ's are averaged) are much less than 4000 keV. Pappalardo (Ref. 33) and Gadioli *et al.* (Ref. 32) do not suggest a procedure for determining the uncertainty in Γ_Δ.

$1000 \leq \Delta \leq 1500$ keV in $\Gamma(\Delta)$ for α_0 at 150° (Fig. 21). The $\Gamma_{\Delta i}$'s within such a range were averaged to obtain the Γ_Δ indicated in Table III; and the resultant Γ_Δ is enclosed by parentheses to indicate its dubious significance.

From the graphs of $C(\Delta,0)$ and $\Gamma(\Delta)$ there was no good evidence of intermediate structure. In the few cases (perhaps five or six) where $C(\Delta,0)$ and $\Gamma(\Delta)$ both give some evidence for a second plateau, either of two conditions is true: (1) Δ is so large that FRD effects make the interpretation of the graphs difficult or (2) the coherence widths corresponding to the second plateau differ only slightly from those of the first plateau.

While most Γ_c, Γ_k, and Γ_Δ estimates (Table II) seem to agree within their rather large uncertainties, there does appear to be a systematic trend for $\Gamma_\Delta < \Gamma_k < \Gamma_c$. It should be emphasized that the average value of Γ is nearly the same regardless of whether the levels are assumed to be isolated (Table III) or strongly overlapping (Table II).

N^{14} LEVELS

Table I lists relevant N^{14} levels and their reported J^π and T assignments. It also lists a qualitative evaluation of the relative intensity of corresponding α groups seen in the present measurements. (Groups corresponding to levels $E_x > 8.489$ MeV were identified primarily from counter telescope survey data at $\varphi = 14°$ and 166° for $12 < E_d < 15$ MeV. Hence the intensity rating of groups at higher E_x in N^{14} may not be representative of the total cross sections to these states.) The results of Table I confirm other evidence[35] concerning the nonexistence of N^{14} levels at $E_x = 6.70$, 7.40, and 7.60 MeV; in addition, serious doubt must be expressed concerning the existence of the 6.05-MeV state, which has only been seen by Clayton[36] in the $N^{15}(He^3,He^4)N^{14}$ reaction at one angle: $\varphi = 150°$.

The fact that isospin-forbidden α groups corresponding to $E_x = 9.508$ and 11.23 MeV appear strongly may throw doubt on the $T=1$ assignment of these states. However, they are not clearly resolved from isospin-allowed states at $E_x = 9.129$ and 11.29 MeV, respectively. If the 9.17-MeV state has actually been observed, it should be noted that there is a nearby state ($E_x = 8.979$ MeV) whose J^π assignment might permit isospin mixing via Coulomb forces.

ACKNOWLEDGMENTS

I sincerely thank Professor Hugh T. Richards for his advice and encouragement throughout this project. Discussions with Professor C. H. Blanchard and Professor K. W. McVoy have been helpful and are gratefully acknowledged. The assistance of F. deForest, P. Jolivette, L. Jacobson, F. Rose, and T. Bonner in data taking is greatly appreciated.

[35] B. G. Harvey, J. R. Meriwether, J. Mahoney, A. Bussiere de Nercy, and D. J. Horen, Phys. Rev. 146, 712 (1966).
[36] D. D. Clayton, Phys. Rev. 128, 2254 (1962).